Protein Expression and Purification 159 (2019) 27–33

Contents lists available at ScienceDirect

Protein Expression and Purification

journal homepage: www.elsevier.com/locate/yprep

Cell-free expression, purification and characterization of *Drosophila melanogaster* odorant receptor OR42a and its co-receptor

Jianyong Li, Xingping Liu, Yahui Man, Qian Chen, Di Pei, Wenjian Wu*

Department of Biology and Chemistry, National University of Defense Technology, Changsha, 410000, Hunan, China

ARTICLE INFO

Keywords:
Cell-free protein synthesis system
Ligand-binding analysis
Membrane protein
Olfactory receptor
Piezoelectric biosensor

ABSTRACT

Olfactory receptors (OR), a group of classic membrane proteins, plays a vital role in insect reproduction and acclimatization. Deciphering the molecular mechanism of insect olfaction could enhance pest control and environmental protection. Studies on ORs have faced a major bottleneck due to the notoriously strong hydrophobicity of ORs, which results in difficult expression in heterologous cell systems. Here, we demonstrated that insect ORs could be functionally produced using the *E. coli* cell-free protein synthesis system (CFPS), in which the highest yield of total ORs is 350 μg per 1 ml reaction. We tested the effects of detergent types and concentrations on soluble expression of ORs. The ORs showed a classic α-helical infrared spectrum. Quartz crystal microbalance (QCM) was used to demonstrate that ORs fold correctly and respond to their ligands. This is the first report that insect OR42a could be functionally produced *in vitro*. This approach may facilitate the development of biomimetic olfactory biosensors and may also be utilized for drug positioning and development, environmental protection and agriculture.

1. Introduction

Membrane proteins account for approximately one third of all sequenced genomes and are involved in many important physiological activities, including transporting substances into or out of cells as a carrier, serving as a specific receptor for hormones, and facilitating cell recognition, signal transduction and cell-to-cell interactions. The significance of membrane proteins is self-evident as they comprise approximately 50% of the targets for drugs and agents in clinical trials [1]. However, information of their structure-function relationship is still limited due to difficulties in obtaining enough purified proteins. Until March 2019, only 872 known structures of unique membrane proteins were reported among a total of 149,600 resolved protein structures (Protein Data Bank). The development of membrane protein structure-function relationship research has been hindered by the notoriously strong hydrophobicity of membrane proteins. Membrane proteins have become an essential part of protein science, structural biology and medical fields because of their extremely critical biological and medical significance. Membrane protein research is also the foundation of biomimetic film and sensing technologies, which have significant theoretical and practical values in the environment and medicine. Novel and efficient methods to produce high-yield and stable, functional membrane protein are imperative.

A wide variety of membrane proteins predominantly comprised of olfactory receptors with seven transmembrane segments function in the olfactory signaling pathway. Vertebrate ORs are one of the evolutionarily oldest sensory membrane proteins and belong to the G-protein coupled receptor (GPCR) family [2,3]. However, insect ORs are primarily expressed on the antennae, and the olfactory signal pathway is independent of GPCRs in insects. Insect ORs themselves can both identify odorant molecules and simultaneously act as ion-gated channels [4,5]. The C-terminus of the insect OR is extracellular, while the N-terminus is intracellular, which is opposite to the vertebrate OR topological structure [6]. The ORs complex in insects are mainly composed of other ORs and co-receptor (ORCO), which often acts as a chaperone [7].

While increasing studies on insect ORs have been carried out, the structure-function relationship and olfactory recognition code are still poorly understood at the molecular level [8,9]. There are no resolved three-dimensional structures for insect ORs. Amino acid coevolution was performed to predict insect ORCO three dimensional structure and ligand binding sites [9]. An additional insect OR agonist ORCORAM2 was reported to produce stronger responses to odorants [10]. A total of 195 residues between extracellular loop 2 and transmembrane domain 4 have been characterized as determinant of odour sensitivity in *Anpheles gambiae* OR15 [11,12]. Nichols and colleagues showed that

* Corresponding author. No. 109 Deya Road, Kaifu District, Changsha City, Hunan Province, China.
E-mail address: wjwu67@126.com (W. Wu).

https://doi.org/10.1016/j.pep.2019.03.001
Received 15 September 2018; Received in revised form 6 January 2019; Accepted 1 March 2019
Available online 11 March 2019
1046-5928/

residues 146–150 located between transmembrane segment 3 and extracellular loop 2 played a key role in odorant recognition in *Drosophila melanogaster* OR85b, while another study demonstrated that a single alanine mutation in transmembrane segment 3 can disturb the odorant activation of moth OR3 [13,14]. Eight amino acid residues at the C-terminus of *Culex quinquefasciatushad* OR8 respond to odorant sensitivity [15]. The second transmembrane domain of *Drosophila melanogaster* OR59b and the second extracellular loop of *Anopheles gambiae* OR10 are involved in odorant response [16,17]. There is seldom another publication to unveil insect ORs structure-function relationship to the best of our knowledge.

Many obstacles emerged during attempts at heterologous expression to produce functional ORs due to the strong hydrophobicity of ORs. Only a few ORs, including OR2AG1, OR226 and ODR10, have been successfully expressed by heterologous *E. coli*, yeast or HEK-293 cells, which falls far behind progress on other protein families [18–20]. Some of these ORs have no biological activity and low expression efficiency due to misfolding [21]. The heterologous overexpression of ORs destroys the cytoplasmic membrane structure and impedes fluid mosaic model; these effects interfere with host cell metabolism and membrane location [22]. Some heterologous expression studies have been delayed mainly derived from insufficient expression and purification of insect ORs. The challenges associated with heterologous expression can be overcome with a CFPS because of its openness and cellular independence [23]. CFPS is an *in vitro* system for protein synthesis, which mainly employs mRNA or DNA as a template and accomplishes protein synthesis with enzymatic reactions in cell extract derived from Sf9 insect cells, *E. coli*, wheat germ and rabbit reticulocyte cells [24,25]. In recent years, researchers have successfully expressed a few kinds of insect ORs *in vitro* by combining surfactants with the significant advantages of CFPS. The solubility rates of *Drosophila melanogaster* OR85b and OR67a were approximately 80% or higher in the *E. coli* cell-free system, while they were nearly insoluble when expressed by heterologous systems [26]. Furthermore, the increased surface area of lipids or nanodiscs allowed for high-efficient, spontaneous membrane insertion of *Drosophila melanogaster* OR22a, OR35a and OR43b [27].

Here, we show high-efficiency functional expression of full-length *Drosophila melanogaster* ORCO and OR42a using an *E. coli* CFPS. Infrared spectra and quartz crystal microbalance demonstrated that ORs featured proper secondary structure and ligand-binding activity. OR production may facilitate the development of membrane protein-based ligand-binding in the future.

2. Materials and methods

2.1. Generation of expression template

The ORCO and OR42a genes were cloned from cDNA of antenna of Canton-S strain of *Drosophila melanogaster*. A 3′ NcoI site and a 5′ SmaI site were added to the ORCO gene by PCR (Forward: CATGCCATGGC AACCTCGATGCAGCCGA; Reverse: TCCCCCGGGTTACTTGAGCTGCAC CAGCACCATAAA). A 3′ NdeI site and a 5′ XhoI site were added to OR42a gene (Forward: GGGAATTCCATATGGATCTGCGAAGGTGGTTT CCG; Reverse: CCGCTCGAGCTCTTCCATTTCAGATTTGGCAAGTTTC). The PCR products were cloned into the pIVEX2.3d and pIVEX2.4d vectors according to manufacturer's instructions (5PRIME, USA). DH5α *E. coli* were transformed with the recombinant plasmid (Tiangen, China), and a single colony was picked to culture overnight. The plasmid DNA encoding ORCO and OR42a was extracted with a commercial kit (Tiangen, China) and verified by Sanger sequencing. Linear expression templates were constructed by two round overlap PCR using Mega primers (Table. S1).

2.2. Cell-free protein synthesis in E. coli CFPS

The components of the cell-free reaction included: 13.3 μg/ml plasmid DNA template; 57 mM HEPES-KOH (pH 7.5); 12 mM magnesium acetate; 80 mM ammonium acetate; 90 mM potassium glutamate; 2 mM Dithiothreitol (DTT); 1.2 mM ATP; 0.85 mM each of CTP, GTP and UTP; 34 μg/ml folinic acid; 67 mM creatine phosphate; 2% PEG8000; 1.0 mM each of 20 amino acids; 3.2 U/ml creatine kinase; 0.01 mM L-[U-^{14}C] leucine (11.1 GBq/mmol); and 27% (v/v) S12 extract [28]. The S12 extract was derived from BL21 Star DE3 *E. coli* according to previously reported methods [29]. The 5 ml reaction was incubated at 30 °C for 3 or 4 h. When the production process was complete, the reaction mix was centrifuged at 12,000 g for 20 min at 4 °C to separate into soluble and insoluble proteins. The separation from input radioactivity was performed by TCA-precipitation. The amount of synthesized ORs was measured by a Tri-Carb 2810 TR scintillation counter (PerkinElmer, Waltham, USA) [30]. L-[U-^{14}C] leucine was added only for quantitative assay. All tests were repeated 3–5 times.

Nine kinds of zwitterionic or nonionic detergents (OG, OTG, DDM, Brij35, Brij58, CHAPS, FC10, FC12, digitonin) were added to the reaction mix at the start of reaction to test the effects of different detergents on soluble and total OR production (Thermo Fisher Scientific and Anatrace, USA). The working concentrations of each detergent were beyond the critical micelle concentration (CMC) and were referenced in previous publications [31,32]. The 5-fold, 9-fold, 20-fold, 50-fold and 100-fold CMCs of Brij35 and Brij58 were used to screen for the optimal concentration to maintain OR solubility.

2.3. Purification of soluble ORs

Purification of soluble, His-tagged ORs was carried out by Ni-NTA (GE healthcare, USA) slurry immunoaffinity chromatography. Soluble ORs were mixed with binding buffer (20 mM sodium phosphate, 500 mM sodium chloride, 10 mM imidazole, and 0.099% (v/v) Brij35, pH 7.0) and Ni-NTA slurry for 2 h at 4 °C. The total mixture was transferred into Ni-NTA column and washed twice with wash buffer (20 mM sodium phosphate, 500 mM sodium chloride, 50 mM imidazole, and 0.099% (v/v) Brij35, pH 7.2). The elution was performed with 5 bed volumes of elution buffer (20 mM sodium phosphate, 500 mM sodium chloride, 300 mM imidazole, and 0.099% (v/v) Brij35, pH 7.2), and the sample was concentrated with a 10 kDa molecular weight cut-off (MWCO) centrifugal filter column (Millipore, USA).

The final purification was performed by size exclusion chromatography (SEC) with a HiPrep 16/60 Sephacryl S-100 HR column using the Akta chromatography system (GE Healthcare, USA). The ORs were loaded and run at 0.5 ml/min with exclusion buffer (50 mM sodium phosphate, 150 mM sodium chloride, and 0.099% (v/v) Brij35, pH 7.2). The collected peak fractions were concentrated for further analysis with SDS-PAGE and Western blot.

2.4. SDS-PAGE and western blot detection of his-tagged ORs

Samples were mixed with NuPAGE loading buffer and incubated at ambient temperature for 20 min. The prepared ORs and prestained or His-tagged protein ladder (Thermo Fisher Scientific, USA) were loaded onto a Novex 4–12% Bis-Tris SDS-PAGE gel (Invitrogen, USA), and run at 150 V for 40 min. Coomassie Brilliant Blue R-250 was employed for protein stains. For blotting, the resolved samples were transferred to a 0.45-μm polyvinylidene difluoride (PVDF) membrane (Millipore, USA) by semidry electrophoretic transfer at 2.5 mA/cm^2 for 45 min. The blots were blocked at room temperature for 1 h in blocking buffer (Thermo Fisher Scientific, USA), incubated with an anti-His polyclonal mouse HRP-conjugated antibody (1: 5000 in Tris-buffered saline with Tween-20, 1 h, room temperature), and visualized by SuperSignal West Pico Luminol/Enhancer Solution (10 min, room temperature). The images were captured using a C-Digit Blot Scanner (LI-COR-USA).

2.5. Secondary structural analysis by fourier transform infrared spectroscopy (FTIR)

The secondary structure of proteins can be characterized by a combination of FTIR and multivariate analysis [33,34]. The spectrum was measured by FTIR using an Attenuated Total Reflectance (ATR) accessory (PerkinElmer, USA). The membrane protein buffer was substituted with D_2O (Sigma, USA) so that the solvent was not detected in the amide I region. The ATR crystal was cleaned with ethanol to eliminate contaminants. The spectrum assay was carried out from 4000 to 500 cm^{-1} with 4 cm^{-1} resolution and 64 scans per spectra [35,36].

The second-derivative and Fourier self-deconvolution (FSD) amide I band (1700 cm^{-1} to 1600 cm^{-1}) were employed to determine the abundance of various structures. The FSD analysis was carried out with Omnic 8.2 with the Happ-Genzel aperdization function. The function was set to 13.0 cm^{-1} full width at half-height and 1.8 enhancement factor, and smoothing points were performed to remove possible white noise during the hierarchical cluster analysis [37]. Further fitting of the spectra was achieved with Peakfit 4.1.2 using the nonlinear least squares so that the center of the derivative curve indicated different content. The relative content of each structure type was measured with Origin 8.0.

2.6. Quartz crystal microbalance odorant binding assay

QCM is a strong tool to test OR binding sensitivity to odorants [38]. The ligand-binding analyses were performed by using the QCM200 piezoelectric biosensor equipped with a 5 MHz, 1-inch diameter, AT-cut quartz crystal (SRS, USA). The crystals were cleaned with UV/ozone for 10 min and then immersed into wash buffer (30% hydrogen peroxide: 25% ammonia: deionized water, 1: 1: 5 v/v) for 5 min at 75 °C to eliminate organic materials and contaminations. The QCM crystals were immediately rinsed with deionized water and dried with nitrogen before the measurement. Membrane protein were immobilized with a combination of aptamers and thiol-dependent, self-assembled monolayers (SAM). The thiol group of the membrane protein cysteine residues bound to gold surface by chemisorption [39]. The QCM crystals were immersed in binding buffer including thiol-decorated anti-His aptamer (5′—HS-$(CH_2)_6$-GGCTTCAGGTTGGTCTGGTTGGGTTTGGCTCC TGTGTACG-3′) for 20 h to develop the SAM [38]. The gold electrodes were rinsed and dried for further research. The purified membrane protein solvent was exchanged with running buffer (10 mM sodium phosphate, 1.8 mM potassium phosphate, 137 mM sodium chloride, 2.7 mM potassium chloride, 3% DMSO, 0.099% Brij35, pH7.6) and 5 μg of protein sample was coated on the center of the pretreated electrode of the gold quartz crystal for 2 h at ambient temperature. The final ratio of ORCO to OR42a was set at 1:1 in the mixture. To remove excess depositions, the QCM sensors were rinsed and dried completely.

The propyl acetate (Sigma, USA) odorant is regarded as a specific ligand for the coreceptor-dependent OR42a in *Drosophila* larva [40]. Propyl acetate gas was prepared using liquid injection and the concentration was defined by the gas-liquid equation:

$$Cg,\ ppm = \frac{10C_lVdRT}{MV_cP}$$

where C_l is the odorant concentration in the solution (wt. %), V is the injected volume, d is the density (g/ml), R is the gas constant, T is the chamber temperature (K), M is the propyl acetate molecular weight (g/mol), V_c is the chamber volume, and P is the pressure in chamber (atm) [41]. Pipeline purging and application of the negative control were done with fresh air. The gas flow rate was set at 0.5 ml/s with a necessary 30 s introduction. The retention time was 120 s, while the purging time was 50 s. Concentration ranging from 5 ppm (v/v) to 150 ppm (v/v) propyl acetate were tested for the sensitivity assay.

The activity the of QCM crystals in response to propyl acetate was detected by the change in frequency at room temperature. The frequency change of the crystals was related to the mass change per area at the electrode, which was indicated by the Sauerbrey equation [42]:

$$\Delta f = -C_f \Delta m$$

where Δf is the observed frequency change (Hz), C_f is the sensitivity factor of the crystal (56.6 Hz/μg cm^2), and Δm is the change in mass per unit area in g/cm^2. The baseline frequency is the frequency in fresh air during stabilization. ΔF_0 indicates the frequency change when the protein coated onto the QCM sensors. ΔF_1 presents the frequency change after applying the gas ligand to the coated QCM crystals. $\Delta F_1/\Delta F_0$ reveals the sensitivity of the ligand and receptor. All measurements were repeated 5–6 times.

3. Results and discussion

3.1. Preparation and screening of expression template

Both linear and plasmid templates were constructed to produce the olfactory receptor in *E. coli* cell-free system. A T7 promoter, T7 terminator and a carboxyl- or amino-terminal six-residue histidine tag were added to the expression templates (Fig. S1). OR42a cloned into the pIVEX2.3d vector with a C-terminal 6x His-tag was successfully produced in the *E. coli* cell-free system, while the version in the pIVEX2.4d vector was not detected. However, ORCO preferred the pIVEX2.4d vector rather than the pIVEX2.3d vector, which indicated its expression level was affected by the position of the tag (Table 1) [43]. Recombinant plasmids were sequenced with dideoxy chain-termination method. Plasmid templates had more efficient OR42a and ORCO expression than linear templates, which was consistent with previous reports [32]. To obtain higher yields of proteins, we used pIVEX2.3d for OR42a and pIVEX2.4d for ORCO. However, linear templates have been commonly used in transcription-translation analysis in cell-free systems for their rapid synthesis and low cost [44]. Both DNA templates and detergents are crucial to final yields.

3.2. Effect of detergent type and concentration for cell-free olfactory receptor expression

The nine detergents listed in Material and Methods are efficient for GPCR solubilization in mammalian cells [45,46]. The final concentrations, which were above their CMCs, are shown in Table S2. Fig. 1 indicated the effects of detergent type and concentration on olfactory receptor extraction levels. DDM, Brij35 and Brij58 increased OR42a production, while FC10, FC12 and CHAPS decreased its levels (Fig. 1A). Brij35, Brij58 and digitonin promoted higher ORCO yield (Fig. 1B) in accord with previous reports [26,27]. OG and OTG had no obvious effect on OR42a and ORCO cell-free production, which agrees with the finding that different detergent types have various effects on GPCR production levels [32,47]. DDM, Brij35, Brij58 and digitonin were screened to optimize the detergent concentration for soluble olfactory receptor expression (Fig. 1C and D).

The DDM mix was chosen to analyze the GPCR 3D structure [48]. Detergents at the proper concentration improved yields by solubilizing proteins. The combination of the cell-free system and a proper detergent may facilitate protein 3D-structure determinations. The rapid and cost-saving cell-free system provided alternative to the

Table 1
Effects of DNA templates on olfactory receptor expression.

	Linear	pIVEX2.3d	pIVEX2.4d
ORCO (μg/ml)	75	*	259
OR42a (μg/ml)	116	350	*

* Non-detectable.

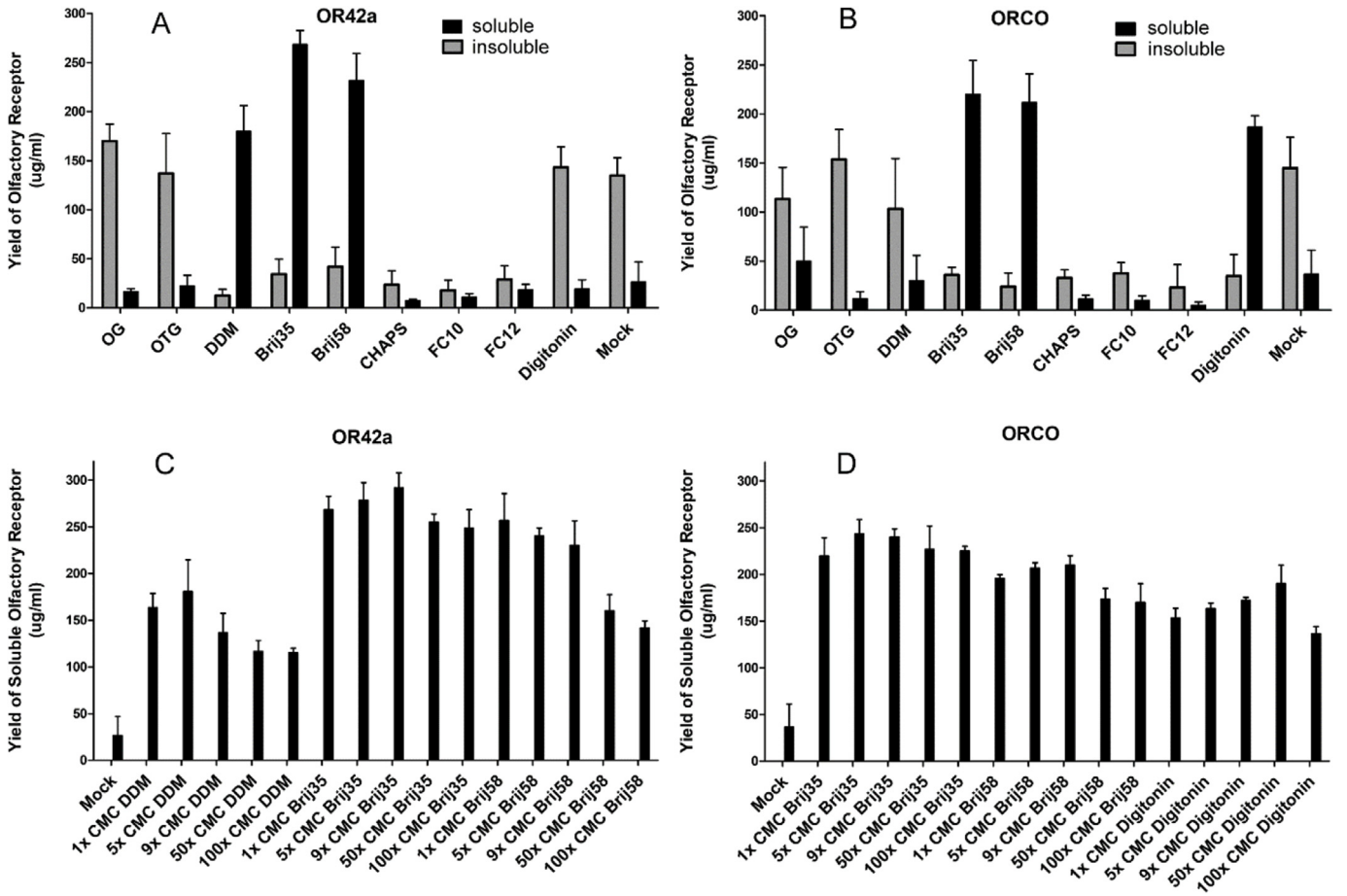

Fig. 1. Effects of detergent type and concentration on olfactory receptor expression. (A and B) The yields of soluble (black) and insoluble (gray) OR42a and ORCO affected by detergents. Mock, no detergent. (C) The soluble production of OR42a with different concentrations of DDM, Brij35, Brij58. (D) The soluble amount of ORCO with different concentration of Brij35, Brij58 and digitonin. Error bars show ± S.E.M. N = 3–5.

heterologous system. Excessive concentrations of detergents that over optimal points may decrease the soluble protein yields possibly through interference of ribosomes. Nine-fold CMC (0.099%) for Brij35 was the most effective detergent with a 95% solubilization rate (Fig. 1). The highest yield of OR42a was 350 μg per 1 ml reaction, which holds promise to help structure-function research. In addition to detergents, the membrane protein yield and stability may be further increased by fusing binding partners together in templates [48].

Several vertebrate ORs have been reported functionally expressed by CFPS, including mOR23, mOR33, mOR103, mOR106, hOR107 and hOR17-4 [32,49]. Those ORs were soluble when expressed with proper detergents. Among detergents, Brij35 and analogues seemed to perform excellent capacity to solubilize ORs, which were also used in our experiment. The average yields were approximate 500 μg per 1 ml reaction, which were comparable with our results. In addition, *Drosophila melanogaster* OR67a and OR85a were also demonstrated to be produced by commercial cell-free system kit [26]. Currently, many soluble proteins have been characterized by CFPS except ORs [50,51].

3.3. Detection and purification of olfactory receptors

Purified protein samples were required for further studies after expression. SDS-PAGE and Western blot analyses were performed to confirm the olfactory receptor expression (Fig. 2). The proteins ran at lower molecular weights on the gels (46 kDa for ORCO and 35 kDa for OR42a) than predicted (54 kDa for ORCO and 47 kDa for OR42a), which was not contradictory to previous studies [52]. ORCO was reported to run at approximately 49 kDa in an insect expression system and wheat germ cell-free system [27]. Faster migration of membrane protein on gels is assumed to be caused by refolding or partial denaturation [52].

The SDS-PAGE analysis in Fig. 2 showed purified ORCO and OR42a with the same sizes as in the Western blot. The peaks in SEC and single bands in the Western blot and SDS-PAGE analyses demonstrated monomeric ORCO and OR42a (Fig. S2). The solubilization and stability of the olfactory receptors may result from additional Brij35 in the elution buffer. Some membrane proteins tended to form aggregates even when efforts were made to avoid this problem [53–56,]. Homodimerization or aggregates should be eliminated for single molecular activity detection of membrane protein. Only correctly fold can proteins have proper functions.

3.4. Secondary structure analysis by FTIR

The amide I (1700 cm^{-1} to 1600 cm^{-1}) absorption of FTIR spectra was used to determine the protein secondary structure [35,37,57]. β-sheet structures are centered at approximately 1630 cm^{-1}, coils at approximately 1642 cm^{-1}, α-helices at approximately 1654 cm^{-1}, β-turns at approximately 1663 cm^{-1}, anti-parallel β-sheets at approximately 1680 cm^{-1}, and side-chains at approximately 1618 $cm^{-1}$and 1690 cm^{-1} [58]. α-helix conformation dominated ORCO and OR42a secondary structures (Fig. 3), which agreed with the report 60% α-helix content in some GPCRs and olfactory receptors [9,26,59]. The integrated area of respective curves presented the relative amount of each conformation. For ORCO, α-helices accounted for 66%, β-sheets 5%, and coils 20%. α-helices accounted for 71% of OR42a, β-turns 4%, and

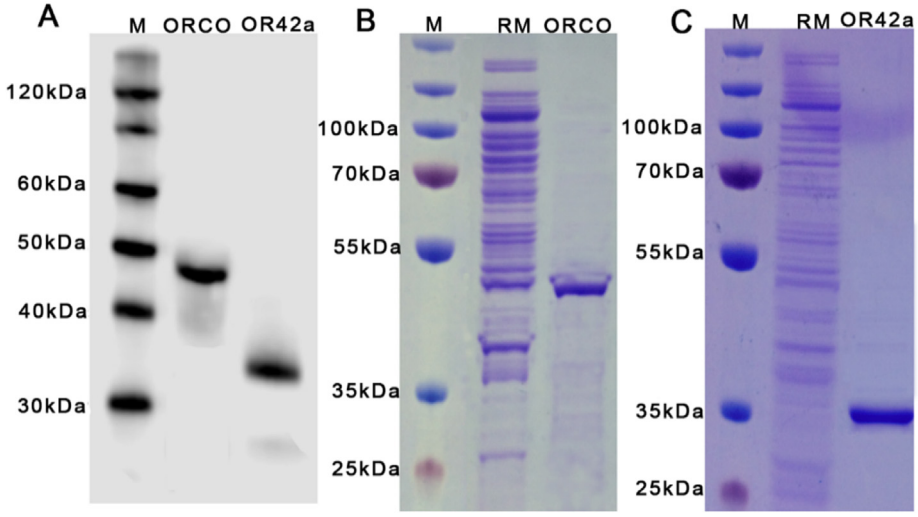

Fig. 2. SDS-PAGE and Western blot detection of olfactory receptors. (A) Western blot for ORCO and OR42a. M, the markers of His-tagged protein ladder. A single ORCO band is detected at approximately 46 kDa, and OR42a at 35 kDa. (B and C) The Coomassie Brilliant Blue stains of purified ORCO and OR42a. M, markers of prestained protein ladder. RM, the reaction mixture. (For interpretation of the references to colour in this figure legend, the reader is referred to the Web version of this article.)

coils 21%. No obvious peaks were detected in the 1625 cm^{-1} or 1695 cm^{-1}, indicating an absence of aggregation. Circular dichroism has been frequently used to analyze the secondary structures of aqueous proteins. FTIR has become a powerful and reliable tool to detect protein secondary structure in both solid and liquid phase. The FWHH and enhancement factor were two pivotal parameters in FTIR spectra analysis. With proper settings, the adjusted r^2 was approximately 1 and sum of squares came from error (SSE) was minimized. In summary, ORCO and OR42a were mainly composed of α-helix conformations as detected by FTIR. The proper secondary structures were foundation of ligand-binding of ORCO and OR42a.

3.5. QCM detection of olfactory receptor ligand binding

The sensitivity of ORCO and OR42a ligand binding was characterized with 90 ppm propyl acetate gas; 5–150 ppm propyl acetate gas was used to analyze the limiting concentration and correlation between ligand and sensitivity. To accurately estimate the response per unit area of QCM sensors, $\Delta F_1/\Delta F_0$ was used to describe the related sensitivity. As shown in Fig. 4 and Fig. S2, only the combination of ORCO and OR42a could respond to the odorant, which conformed to the insect olfactory receptor heteromeric theory [5]. The gas retention area indicated a stable ligand binding response. Neither ORCO nor OR42a could recognize the ligand as evaluated by QCM when alone (Fig. 4). The heterodimer model and role of ORCO in recognizing odorants was recently demonstrated in *Drosophila* larvae [60]. The latest reports claimed that the ORCO and ORx heterodimer is activated by agonists *in vivo* [10]. Our results suggested that ORCO and OR42a may form herterodimer or multimer *in vitro*. QCM was expected to be a promising tool for deciphering the olfactory code. The correlation of ligand concentration and sensitivity exhibited a linear response (Fig. 4). An accurate amount of molecular binding can be calculated from the linear equation. Stable repeat cycles were observed from the QCM sensor coated with ORCO and OR42a responding to a 90-ppm odorant (Fig. S2). The frequency shift of ± 1 Hz between the baselines of each cycle probably stemmed from incomplete odorant exclusion or inevitable mechanical error. The reproducibility was lessened when the gas concentration exceeded the range of 5–120 ppm, which may have been due to the thin-film deposits required by the Sauerbrey equation [61].

The frequency change was approximately 152 Hz after coating the aptamer with His-tagged protein. The maximum frequency change was approximately 33 Hz after ligand binding, indicating that the aptamer facilitated absolute sensitivity compared with physical adsorption [38,62]. The effective modification of QCM crystals may generate better capacity. The results showed that membrane protein interaction and ligand-binding could be detected by a piezoelectric biosensor.

4. Conclusions

This study evaluated the production of olfactory receptors from an

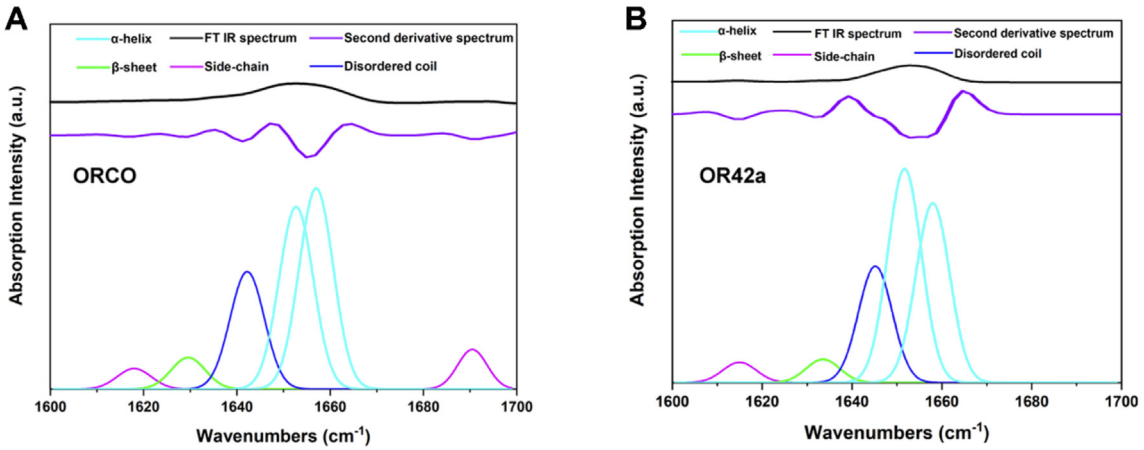

Fig. 3. Fourier transform infrared spectroscopy analysis of olfactory receptors. (A and B) FTIR spectrum (black) and second derivative spectrum (violet) as long as the secondary structure components (colour) of ORCO and OR42a. (For interpretation of the references to colour in this figure legend, the reader is referred to the Web version of this article.)

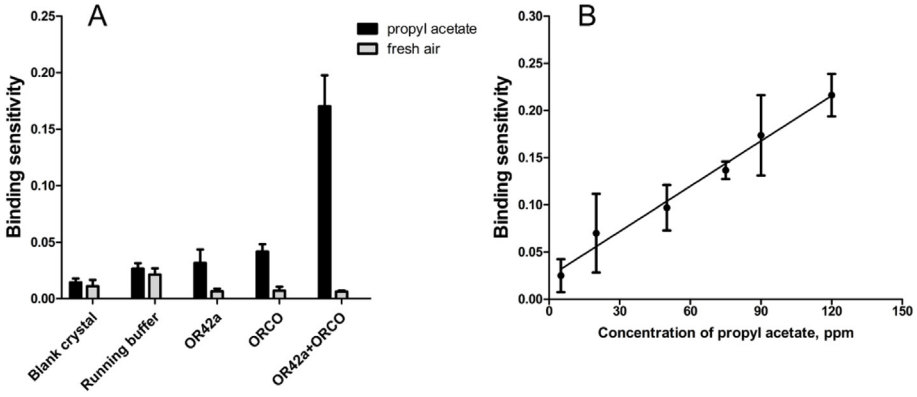

Fig. 4. QCM sensor responses to odorant. (A) QCM responses of ORCO and OR42a to propyl acetate (black) and fresh air (gray). Blank crystal, vacant QCM crystal. Running buffer, only running buffer coated onto QCM sensor. OR42a, QCM sensor coated with OR42a. ORCO, QCM sensor coated with ORCO. OR42a + ORCO, QCM sensor coated with OR42a and ORCO. (B) Dose-dependent QCM responses to propyl acetate. Binding sensitivity shows a linear correlation to concentration. Error bars show ± S.E.M. N = 5–6.

E. coli cell-free protein synthesis system, which tended to be a potential tool to synthesize functional membrane proteins. The OR42a olfactory receptor was characterized *in vitro* for the first time. A systematical screen of detergents was used to solubilize and purify membrane proteins. In addition, the high yield and purity hold promise for characterization of the three-dimensional structure in the future. Membrane proteins produced by a cell-free system combined with detergent had proper folding and ligand binding capacity.

Further studies need to be performed to analyze binding sites and structure. Cell-free may be a viable option for membrane protein ligand-binding. Membrane protein-based piezoelectric biosensors will likely be applied towards environmental protection, signal transduction and biomimetic research.

Conflicts of interest

The authors declare that they have no conflict of interest.

Acknowledgements

We thank Professor Dong-Myung Kim, for his providing the CFPS components and detailed guidance. We thank Dr. Justin Watkins for manuscript assistance.

Appendix A. Supplementary data

Supplementary data to this article can be found online at https://doi.org/10.1016/j.pep.2019.03.001.

References

[1] A.S. Hauser, M.M. Attwood, M. Rask-Andersen, H.B. Schioth, D.E. Gloriam, Trends in GPCR drug discovery: new agents, targets and indications, Nat. Rev. Drug Discov. 16 (2017) 829–842.
[2] R.C. Araneda, A.D. Kini, S. Firestein, The molecular receptive range of an odorant receptor, Nat. Neurosci. 3 (2000) 1248.
[3] L. Buck, R. Axel, A novel multigene family may encode odorant receptors: a molecular basis for odor recognition, Cell 65 (1991) 175–187.
[4] D. Wicher, R. Schafer, R. Bauernfeind, M.C. Stensmyr, R. Heller, S.H. Heinemann, B.S. Hansson, Drosophila odorant receptors are both ligand-gated and cyclic-nucleotide-activated cation channels, Nature 452 (2008) 1007–1011.
[5] K. Sato, M. Pellegrino, T. Nakagawa, T. Nakagawa, L.B. Vosshall, K. Touhara, Insect olfactory receptors are heteromeric ligand-gated ion channels, Nature 452 (2008) 1002–1006.
[6] C. Lundin, L. Kall, S.A. Kreher, K. Kapp, E.L. Sonnhammer, J.R. Carlson, G. Heijne, I. Nilsson, Membrane topology of the Drosophila OR83b odorant receptor, FEBS Lett. 581 (2007) 5601–5604.
[7] M.C. Larsson, A.I. Domingos, W.D. Jones, M.E. Chiappe, H. Amrein, L.B. Vosshall, Or83b encodes a broadly expressed odorant receptor essential for Drosophila olfaction, Neuron 43 (2004) 703–714.
[8] Z. Wang, P. Yang, D. Chen, F. Jiang, Y. Li, X. Wang, L. Kang, Identification and functional analysis of olfactory receptor family reveal unusual characteristics of the olfactory system in the migratory locust, Cell. Mol. Life Sci. 72 (2015) 4429–4443.
[9] T.A. Hopf, S. Morinaga, S. Ihara, K. Touhara, D.S. Marks, R. Benton, Amino acid coevolution reveals three-dimensional structure and functional domains of insect odorant receptors, Nat. Commun. 6 (2015) 6077.
[10] P. Tsitoura, K. Iatrou, Positive allosteric modulation of insect olfactory receptor function by ORco agonists, Front. Cell. Neurosci. 10 (2016) 275.
[11] S. Rahman, C.W. Luetje, Mutant cycle analysis identifies a ligand interaction site in an odorant receptor of the malaria vector Anopheles gambiae, J. Biol. Chem. 292 (2017) 18916–18923.
[12] D.T. Hughes, G. Wang, L.J. Zwiebel, C.W. Luetje, A determinant of odorant specificity is located at the extracellular loop 2-transmembrane domain 4 interface of an Anopheles gambiae odorant receptor subunit, Chem. Senses 39 (2014) 761–769.
[13] A.S. Nichols, C.W. Luetje, Transmembrane segment 3 of Drosophila melanogaster odorant receptor subunit 85b contributes to ligand-receptor interactions, J. Biol. Chem. 285 (2010) 11854–11862.
[14] G.P. Leary, J.E. Allen, P.L. Bunger, J.B. Luginbill, C.E. Linn Jr., I.E. Macallister, M.P. Kavanaugh, K.W. Wanner, Single mutation to a sex pheromone receptor provides adaptive specificity between closely related moth species, Proc. Natl. Acad. Sci. U. S. A. 109 (2012) 14081–14086.
[15] S.R. Hill, S. Majeed, R. Ignell, Molecular basis for odorant receptor tuning: a short C-terminal sequence is necessary and sufficient for selectivity of mosquito Or8, Insect Mol. Biol. 24 (2015) 491–501.
[16] P. Xu, W.S. Leal, Probing insect odorant receptors with their cognate ligands: insights into structural features, Biochem. Biophys. Res. Commun. 435 (2013) 477–482.
[17] M. Pellegrino, N. Steinbach, M.C. Stensmyr, B.S. Hansson, L.B. Vosshall, A natural polymorphism alters odour and DEET sensitivity in an insect odorant receptor, Nature 478 (2011) 511–514.
[18] J.Y. Lee, H.J. Ko, S.H. Lee, T.H. Park, Cell-based measurement of odorant molecules using surface plasmon resonance, Enzym. Microb. Technol. 39 (2006) 375–380.
[19] H.S. Song, S.H. Lee, E.H. Oh, T.H. Park, Expression, solubilization and purification of a human olfactory receptor from Escherichia coli, Curr. Microbiol. 59 (2009) 309–314.
[20] V. Radhika, T. Proikas-Cezanne, M. Jayaraman, D. Onesime, J.H. Ha, D.N. Dhanasekaran, Chemical sensing of DNT by engineered olfactory yeast strain, Nat. Chem. Biol. 3 (2007) 325–330.
[21] L. Ivic, C. Zhang, X. Zhang, S.O. Yoon, S. Firestein, Intracellular trafficking of a tagged and functional mammalian olfactory receptor, Developmental Neurobiology 50 (2002) 56–68.
[22] S. Wagner, M.L. Bader, D. Drew, J.-W. de Gier, Rationalizing membrane protein overexpression, Trends Biotechnol. 24 (2006) 364–371.
[23] S.F. Fenz, R. Sachse, T. Schmidt, S. Kubick, Cell-free synthesis of membrane proteins: tailored cell models out of microsomes, Biochim. Biophys. Acta 1838 (2014) 1382–1388.
[24] H. Nakano, T. Yamane, Cell-free protein synthesis systems, Biotechnol. Adv. 16 (1998) 367–384.
[25] F. Katzen, T.C. Peterson, W. Kudlicki, Membrane protein expression: no cells required, Trends Biotechnol. 27 (2009) 455–460.
[26] L.T. Tegler, K. Corin, J. Hillger, B. Wassie, Y. Yu, S. Zhang, Cell-free expression, purification, and ligand-binding analysis of Drosophila melanogaster olfactory receptors DmOR67a, DmOR85b and DmORCO, Sci. Rep. 5 (2015) 7867.
[27] C. Carraher, A.R. Nazmi, R.D. Newcomb, A. Kralicek, Recombinant expression, detergent solubilisation and purification of insect odorant receptor subunits, Protein Expr. Purif. 90 (2013) 160–169.
[28] D. Kasi, C. Catherine, S.W. Lee, K.H. Lee, Y.J. Kim, M. Ro Lee, J.W. Ju, D.M. Kim, Cell-free translational screening of an expression sequence tag library of Clonorchis sinensis for novel antigen discovery, Biotechnol. Prog. 33 (2017) 832–837.
[29] T.W. Kim, J.W. Keum, I.S. Oh, C.Y. Choi, C.G. Park, D.M. Kim, Simple procedures for the construction of a robust and cost-effective cell-free protein synthesis system, J. Biotechnol. 126 (2006) 554–561.
[30] D.M. Kim, J.R. Swartz, Prolonging cell-free protein synthesis by selective reagent additions, Biotechnol. Prog. 16 (2000) 385–390.
[31] C. Klammt, D. Schwarz, K. Fendler, W. Haase, V. Dotsch, F. Bernhard, Evaluation of detergents for the soluble expression of alpha-helical and beta-barrel-type integral membrane proteins by a preparative scale individual cell-free expression system, FEBS J. 272 (2005) 6024–6038.
[32] L. Kaiser, J. Graveland-Bikker, D. Steuerwald, M. Vanberghem, K. Herlihy, S. Zhang, Efficient cell-free production of olfactory receptors: detergent optimization,

structure, and ligand binding analyses, Proc. Natl. Acad. Sci. Unit. States Am. 105 (2008) 15726–15731.
[33] S. Ito, H. Kandori, V.A. Lorenz-Fonfria, Potential second-harmonic ghost bands in fourier transform infrared (FT-IR) difference spectroscopy of proteins, Appl. Spectrosc. 72 (2018) 956–963.
[34] A. Ghosh, J.S. Ostrander, M.T. Zanni, Watching proteins wiggle: mapping structures with two-dimensional infrared spectroscopy, Chem. Rev. 117 (2017) 10726–10759.
[35] H. Yang, S. Yang, J. Kong, A. Dong, S. Yu, Obtaining information about protein secondary structures in aqueous solution using Fourier transform IR spectroscopy, Nat. Protoc. 10 (2015) 382–396.
[36] X. Liu, C. Liang, X. Zhang, J. Li, J. Huang, L. Zeng, Z. Ye, B. Hu, W. Wu, Amyloid fibril aggregation: an insight into the underwater adhesion of barnacle cement, Biochem. Biophys. Res. Commun. 493 (2017) 654–659.
[37] N. Cebi, M.Z. Durak, O.S. Toker, O. Sagdic, M. Arici, An evaluation of Fourier transforms infrared spectroscopy method for the classification and discrimination of bovine, porcine and fish gelatins, Food Chem. 190 (2016) 1109–1115.
[38] L. Du, C. Wu, H. Peng, L. Zou, L. Zhao, L. Huang, P. Wang, Piezoelectric olfactory receptor biosensor prepared by aptamer-assisted immobilization, Sensor. Actuator. B Chem. 187 (2013) 481–487.
[39] A. Ulman, An Introduction to Ultrathin Organic Films: from Langmuir–Blodgett to Self–Assembly, Academic press, 2013.
[40] D. Munch, C.G. Galizia, DoOR 2.0–comprehensive mapping of Drosophila melanogaster odorant responses, Sci. Rep. 6 (2016) 21841.
[41] T. Nakamoto, M. Yosihioka, Y. Tanaka, K. Kobayashi, T. Moriizumi, S. Ueyama, W.S. Yerazunis, Colorimetric method for odor discrimination using dye-coated plate and multiLED sensor, Sensor. Actuator. B Chem. 116 (2006) 202–206.
[42] G. Sauerbrey, Verwendung von Schwingquarzen zur Wägung dünner Schichten und zur Mikrowägung, Z. Phys. 155 (1959) 206–222.
[43] E. Weber, J. Birkenfeld, J. Franz, U. Gritzan, L. Linden, M. Trautwein, Modular Protein Expression Toolbox (MoPET), a standardized assembly system for defined expression constructs and expression optimization libraries, PLoS One 12 (2017) e0176314.
[44] R. Marshall, C.S. Maxwell, S.P. Collins, C.L. Beisel, V. Noireaux, Short DNA containing chi sites enhances DNA stability and gene expression in E. coli cell-free transcription-translation systems, Biotechnol. Bioeng. 114 (2017) 2137–2141.
[45] B.L. Cook, K.E. Ernberg, H. Chung, S. Zhang, Study of a synthetic human olfactory receptor 17-4: expression and purification from an inducible mammalian cell line, PLoS One 3 (2008) e2920.
[46] B.L. Cook, D. Steuerwald, L. Kaiser, J. Graveland-Bikker, M. Vanberghem, A.P. Berke, K. Herlihy, H. Pick, H. Vogel, S. Zhang, Large-scale production and study of a synthetic G protein-coupled receptor: human olfactory receptor 17-4, Proc. Natl. Acad. Sci. Unit. States Am. 106 (2009) 11925–11930.
[47] I.H. Navratilova, T. Aristotelous, L.E. Bird, A.L. Hopkins, Surveying GPCR solubilisation conditions using surface plasmon resonance, Anal. Biochem. 556 (2018) 23–34.
[48] Y. Peng, J.D. McCorvy, K. Harpsoe, K. Lansu, S. Yuan, P. Popov, L. Qu, M. Pu, T. Che, L.F. Nikolajsen, X.P. Huang, Y. Wu, L. Shen, W.E. Bjorn-Yoshimoto, K. Ding, D. Wacker, G.W. Han, J. Cheng, V. Katritch, A.A. Jensen, M.A. Hanson, S. Zhao, D.E. Gloriam, B.L. Roth, R.C. Stevens, Z.J. Liu, 5-HT2C receptor structures reveal the structural basis of GPCR polypharmacology, Cell 172 (2018) 719–730 e714.
[49] K. Corin, P. Baaske, D.B. Ravel, J. Song, E. Brown, X. Wang, S. Geissler, C.J. Wienken, M. Jerabek-Willemsen, S. Duhr, D. Braun, S. Zhang, A robust and rapid method of producing soluble, stable, and functional G-protein coupled receptors, PLoS One 6 (2011) e23036.
[50] S. Yokoyama, Protein expression systems for structural genomics and proteomics, Curr. Opin. Chem. Biol. 7 (2003) 39–43.
[51] S. Yokoyama, T.C. Terwilliger, S. Kuramitsu, D. Moras, J.L. Sussman, RIKEN aids international structural genomics efforts, Nature 445 (2007) 21.
[52] M. Michalik, M. Orwick-Rydmark, M. Habeck, V. Alva, T. Arnold, D. Linke, An evolutionarily conserved glycine-tyrosine motif forms a folding core in outer membrane proteins, PLoS One 12 (2017) e0182016.
[53] A.O. Oluwole, B. Danielczak, A. Meister, J.O. Babalola, C. Vargas, S. Keller, Solubilization of membrane proteins into functional lipid-bilayer nanodiscs using a diisobutylene/maleic acid copolymer, Angew. Chem. Int. Ed. 56 (2017) 1919–1924.
[54] F. Hagn, M.L. Nasr, G. Wagner, Assembly of phospholipid nanodiscs of controlled size for structural studies of membrane proteins by NMR, Nat. Protoc. 13 (2018) 79–98.
[55] H. Oshikane, M. Watabe, T. Nakaki, Facilitation of yeast-lethal membrane protein production by detoxifying with GFP tagging, Protein Expr. Purif. 148 (2018) 40–45.
[56] I. Chamma, O. Rossier, G. Giannone, O. Thoumine, M. Sainlos, Optimized labeling of membrane proteins for applications to super-resolution imaging in confined cellular environments using monomeric streptavidin, Nat. Protoc. 12 (2017) 748–763.
[57] J. Seo, W. Hoffmann, S. Warnke, X. Huang, S. Gewinner, W. Schollkopf, M.T. Bowers, G. von Helden, K. Pagel, An infrared spectroscopy approach to follow beta-sheet formation in peptide amyloid assemblies, Nat. Chem. 9 (2017) 39–44.
[58] A. Barth, Infrared spectroscopy of proteins, Biochim. Biophys. Acta 1767 (2007) 1073–1101.
[59] P.J. Shilling, F. Bumbak, D.J. Scott, R.A.D. Bathgate, P.R. Gooley, Characterisation of a cell-free synthesised G-protein coupled receptor, Sci. Rep. 7 (2017) 1094.
[60] N. Utashiro, C.R. Williams, J.Z. Parrish, K. Emoto, Prior activity of olfactory receptor neurons is required for proper sensory processing and behavior in Drosophila larvae, Sci. Rep. 8 (2018) 8580.
[61] S.I. Boyadjiev, V. Georgieva, N. Stefan, G.E. Stan, N. Mihailescu, A. Visan, I.N. Mihailescu, C. Besleaga, I.M. Szilágyi, Characterization of PLD grown WO 3 thin films for gas sensing, Appl. Surf. Sci. 417 (2017) 218–223.
[62] S. Sankaran, S. Panigrahi, S. Mallik, Olfactory receptor based piezoelectric biosensors for detection of alcohols related to food safety applications, Sensor. Actuator. B Chem. 155 (2011) 8–18.